CHAPTER - 4

ELECTRICAL PROPERTIES.

ELECTRICAL PROPERTIES

INTRODUCTION

Mechanism of charge transport can be understood from the measurements of Electrical conductivity, Thermo-electric power, Hall co.efficient and Magneto-resistance. Density and mobility of charge carriers are the key-quantities for obtaining inner details of the conductivity. The low conductivity compared to metals, greatly influences the various applications of ferrites at microwave frequencies.

Resistivities as low as 10^{-2} ohm-cm are found in iron-rich ferrites[1] and frequency dependent dielectric behaviour[2-5] created considerable interest for understanding many physical and chemical properties.

Verwey attributed high conductivity to the presence of Fe^{2+} and Fe^{3+} ions on equivalent sites.[6] However, Koops[7] attributed it largely to the preparation technique. According to him iron deficiency results in high resistivity while low resistivity is due to excess of iron. Hence iron deficiency material acts as p-type and excess iron material as n-type.

Maizen[8] is one amongst the many investigators who studied conduction mechanism on the basis of band picture and hopping model. Band picture attributes temperature dependence of conductivity to charge carrier concentration. Hopping model considers that conductivity is because of changes in mobility of charge carriers with temperature.

SECTION-A

ELECTRICAL CONDUCTIVITY

4.1. CONDUCTION MECHANISM IN FERRITES

Conventional band theory fails to account for the electrical transport properties in oxides and mechanism of transport phenomenon in ferrites may be represented by,

$Me^{2+}\ O^{2-}\ Fe^{3+} \longrightarrow Me^{3+}\ O^{2-}\ Fe^{2+} + E_{act}$ where, ...(1)

E_{act} = Activation Energy. Verwey et al worked out the mechanism of conduction in $FeO\ Fe_2O_3$. Fe^{2+} and Fe^{3+} ions are at the octahedral site-B, in this structure. The extra electron on Fe^{2+} ion requires very small amount of energy to move towards adjacent Fe^{3+} ion on the same site. The valence states of the two ions get inter-changed. Under the influence of an electric field, these extra electrons constitute the conduction current. The Verwey mechanism then can be shown as,

$$Fe_B^{2+} + Fe_B^{3+} \rightleftharpoons Fe_B^{3+} + Fe_B^{2+} + E_{act} \qquad .....(2)$$

In case of $NiOFe_2O_3$, the mechanism can be,

$Ni_B^{2+} + Fe_B^{3+} \rightleftharpoons Ni_B^{3+} + Fe_B^{2+} + E_{act}$ where, ...(3)

'B' denotes octahedral sites.

Ferrites are semiconducting oxide magnetic materials. Hence conduction mechanism can be considered in terms of electrons and holes. The charge transport is due to the migration of charge carriers under the external potential difference. Ferrites exhibit the decrease in resistivity with increase in temperature according to the relation, $\rho = \rho_0 \exp(Eg/KT)$ where, ...(4)

Eg = activation energy. The activation energy is required to cause the electron jump in conduction mechanism.

The graph of logρ versus 1/T shows a break in curve at transition temperature corresponding to curie temperature. The change in slope is due to disorder of spin at this temperature. It indicates predominant change in conduction mechanism. The values of Eg lie in the range 0.1 to 0.5 eV. The high activation energy is associated with a high resistivity at room temperature.

Van Uitert and Jonker showed the dependence of the resistivity on stochiometry. The presence of excess iron leads to the formation of Fe^{2+} with the reduction in resistivity. For preparation of high resistivity ferrite, excess iron in the lattice is avoided and small quantity of manganese or cobalt is added in a perfectly stochiometric ferrite.

In case of nickel ferrite the presence of manganese makes the process more energetically favourable as,

$Ni^{3+} + Mn^{2+} \longrightarrow Ni^{2+} + Mn^{3+}$ and $Fe^{2+} + Mn^{3+} \longrightarrow Fe^{3+} + Mn^{2+}$....(5)

This process suppresses the formation of divalent iron and trivalent nickel of process[3]. Mn^{2+} and Mn^{3+} present however, are widely separated and require high activation energy for conduction of electrons between them, Mn being kept at low concentration.This enhances the resistivity.

Van Uitert also showed that Ni-Zn ferrites sintered at 1250°C possess the large values of resistivity on polishing the upper surface. However, unpolished samples show considerably small values of resistivity. This he attributed to the zinc which volatalized from the surface encouraging formation of Fe^{2+} ions at the surface layer.

4.2. ELECTRON HOPPING AND POLARONS

An electron interacts with the ions or atoms of lattice and

creates local deformation of lattice. This deformation follows the electron as it moves through the lattice. Due to this, there is an increase in the effective mass of electron in many cases.The combination of the electron together with its strain field is - known as polaron.

Interaction of conduction electron or hole with neighbouring ions may result in a displacement of the ions. Polarization of the surrounding region takes place with the carrier at the centre of a polarization potential well. For deep potential well, trapped - carrier at the lattice site may be transported by thermal activa - tion. This transport of charge carrier is hopping mechanism.Heikes and Johnston[9] have derived an expression for the mobility of a - charge carrier during hopping process as,

$M = (e^2 d^2 w_o / KT)\ Exp(-Eg/KT)$ where, ...(6)

d = distance between the nearest neighbouring sites(Jump length),

e = charge of electron, w_o = phonon frequency and

Eg= activation energy for hopping process.

The strength of lattice-electron interaction is measured by the coupling constant 'α' which is defined as,

$\alpha/2 =$ (deformation energy)$/h W_L$ where, ...(7)

W_L = Longitudinal phonon frequency. The term $\alpha/2$ is treated as the number of phonons, surrounding an electron slowly moving in a crystal. Hence, more the number of phonons surrounding an electron, larger is the size of polaron. Large polarons are found in ionic crystals. Whereas small polaron is formed if electron is trapped by small number of phonons. Such small polarons are found in covalent crystals. Large and small polarons can be explained on the basis of coupling constant 'α'also. The real size of the

polaron can be understood from free energy considerations. Frohlich[10] developed a model of polaron in order to formulate Hamiltonian interaction for large polaron.

At high temperature conduction is due to the electron jumps from one site to next one in analogy with thermal activation - process accounted in ionic diffusion and ionic conductivity.[11,12] At low temperature, conduction is due to slow tunnelling of electrons. At sufficiently low temperature, polaron behaves as a - particle moving in a narrow band. There is strong experimental - evidence for the existence of small polarons and hopping mechanism.[13,14]

4.3. ACTIVATION ENERGY

Energy gap between the top of valence band and bottom of the conduction band in pure semiconductors, measures activation energy. However, in polycrystalline oxide semiconductors, the band picture is not useful and also Bloch wave functions cannot be applied to the almost localized electrons at lattice sites. The concept of activation energy is discussed in a different way.

Ferrite material is assumed to possess different conducting states, which are discrete in nature and are separated by forbidden bands of conduction. Certain minimum energy is necessary for an electron to take a jump from lower state of conduction to higher state of conduction and charge carriers require some external - agency so that they can cross the barrier. Kinetic theory of heat can be used to define thermal activation. The minimum energy required for the charge carriers to just overcome the barrier, making the conduction possible is taken as a measure of activation energy.

Activation is also possible by other agencies like optical wave energy, electric or magnetic fields. The impurities create trap-levels and localised states.[15] Super exchange requires activation of electrons for the purpose of conduction.

4.4. EXPERIMENTAL TECHNIQUE

Resistance was measured by two probe method on compressed and sintered pellets of about 1.5cms in diameter and 0.2cms in thickness with the help of LCR Bridge, at low frequency of 100 Hz and 1 Khz.

Measurements were carried out with the help of a special - sample holder, fabricated in the workshop of physics department of Shivaji University, Kolhapur. It consists of brass electrodes - fitted in porcelein discs. They are provided with the connection leads. To ensure the firm holding of the sample between the electrodes the screws are provided to the brass rods. The sample pellet is first polished and cleaned. The silver paste is applied to both of its surfaces and for good ohmic contact, it is sandwitched properly between the silver plates. The sandwitched pellet is fixed firmly in the sample-holder with the help of screws provided to it. The brass electrode tips are properly polished and checked to have good continuity with negligible contact resistance before the sample being fixed in it.

Entire assembly was kept inside the temperature regulated - furnace. The chromel-alumel thermocouple was used to measure the temperature of pellet, accurately by keeping its one junction very close to the sample. Resistance is noted with the LCR Bridge for 100 Hz and 1 KHz for different temperatures. The thickness 'h' of a pellet and area A are determined, to calculate the resistivity

of the sample by using the formula,

$\rho = \frac{A}{h} . R$ where R is resistance .....(8)

The plots of log ρ versus $\frac{10^4}{T}$ were plotted for various samples to calculate the activation energy and to determine curie temperature for 100 Hz and 1 KHz.

4.5. RESULTS AND DISCUSSION

In figure 4.1, variations of log ρ versus $\frac{10^4}{T}$ are shown, in the temperature range from room temperature to 800°K for the series. The nature of variation is similar in all the samples - and resistivity behaves according to Arrhenius relation,

$\rho = \rho_o \text{ Exp } (Eg/KT)$ where,

Eg = Activation energy, K = Boltzmann constant and

T = Absolute temperature. The distinct breaks are observed in the temperature variation of resistivity, the first break at lower temperature around 100°C remains constant nearly for all samples and at higher temperature break changes with Mn concentrations. This temperature nearly coincides with the curie temperature of - these samples.

Komar and Klivshin[16] have observed changes in the conductivity plots near curie temperature. Verwey et al[17] have observed this type of discontinuity in Mn-Ni ferrites and these discontinuities shifted with respect to Mn content. They observed high activation energy of materials to be due to high resistivity of - the materials at room temperature. Ghani et al[18] have observed - three regions in Cu-Ni ferrites and suggested that the conduction mechanism changes from one region to another region. The conduction in the first region is due to impurity charge carriers, in the

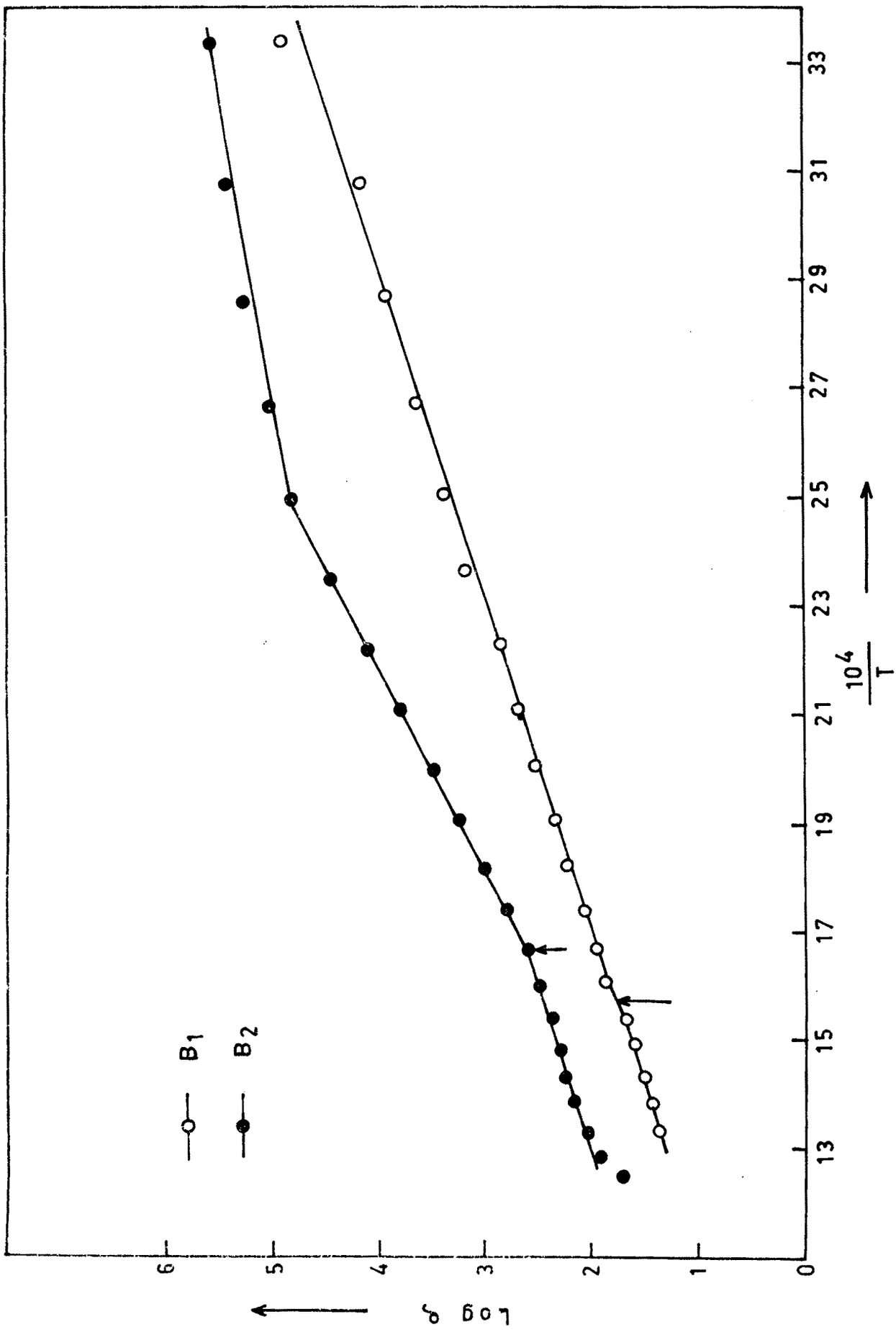

FIG.4.1(a) — VARIATION OF Log ρ WITH $\frac{10^4}{T}$ FOR B_1 AND B_2 WITH 100 Hz.

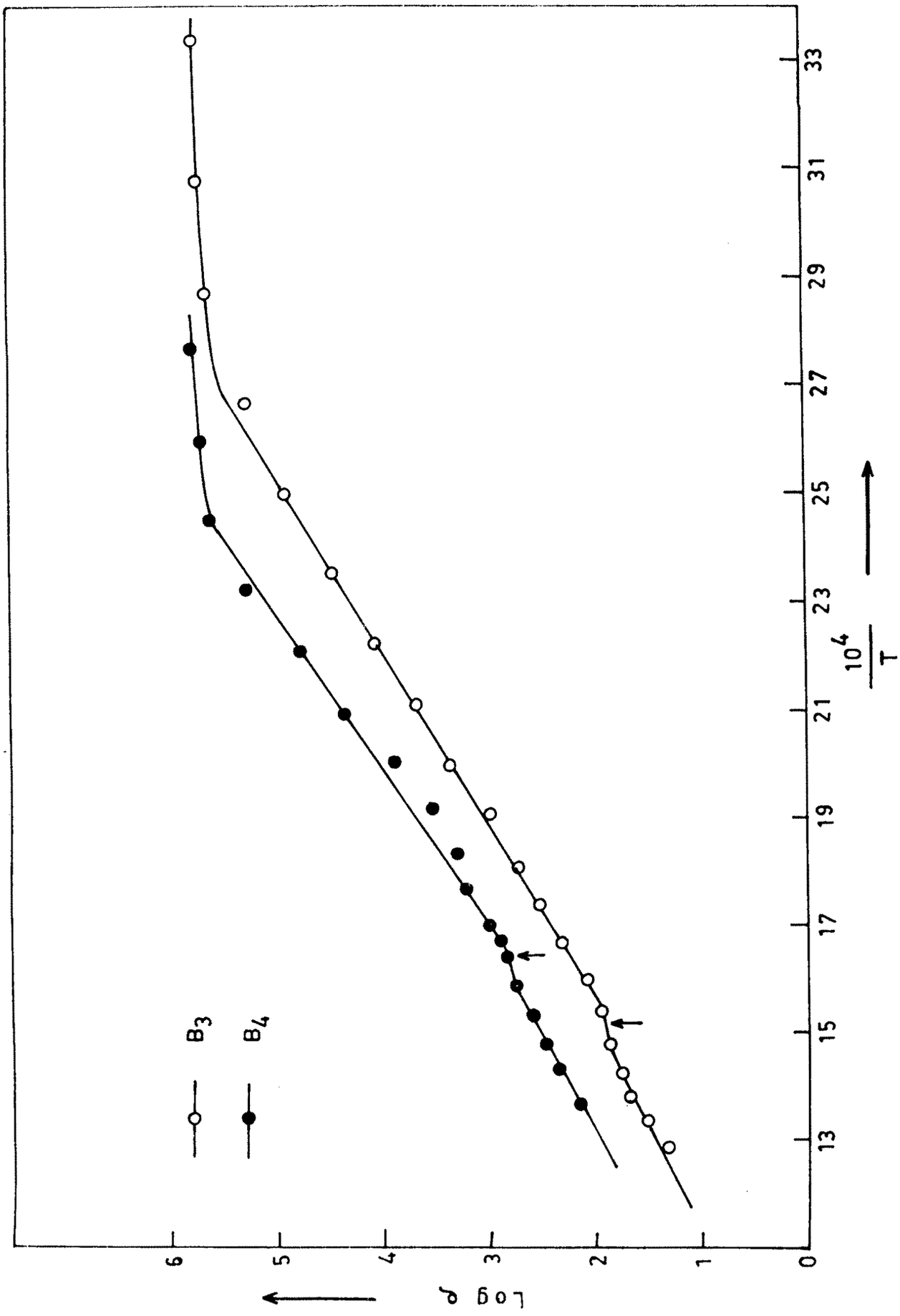

FIG. 4-1 (b) — VARIATION OF Log ρ WITH $\frac{10^4}{T}$ FOR B_3 AND B_4 WITH 100 Hz.

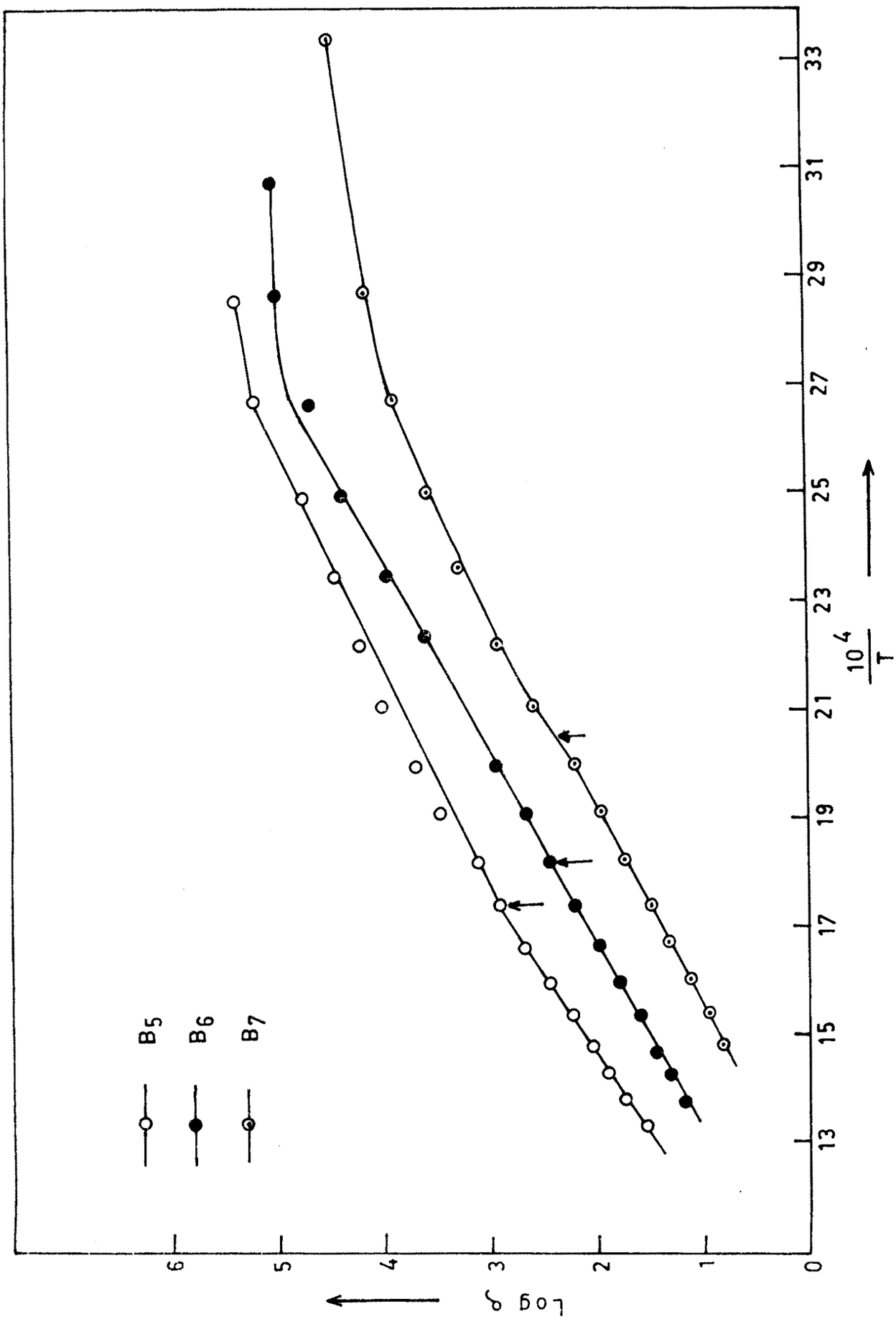

FIG. 4·1(c)—VARIATION OF Log ρ WITH $\frac{10^4}{T}$ FOR B_5, B_6 AND B_7 WITH 100 Hz.

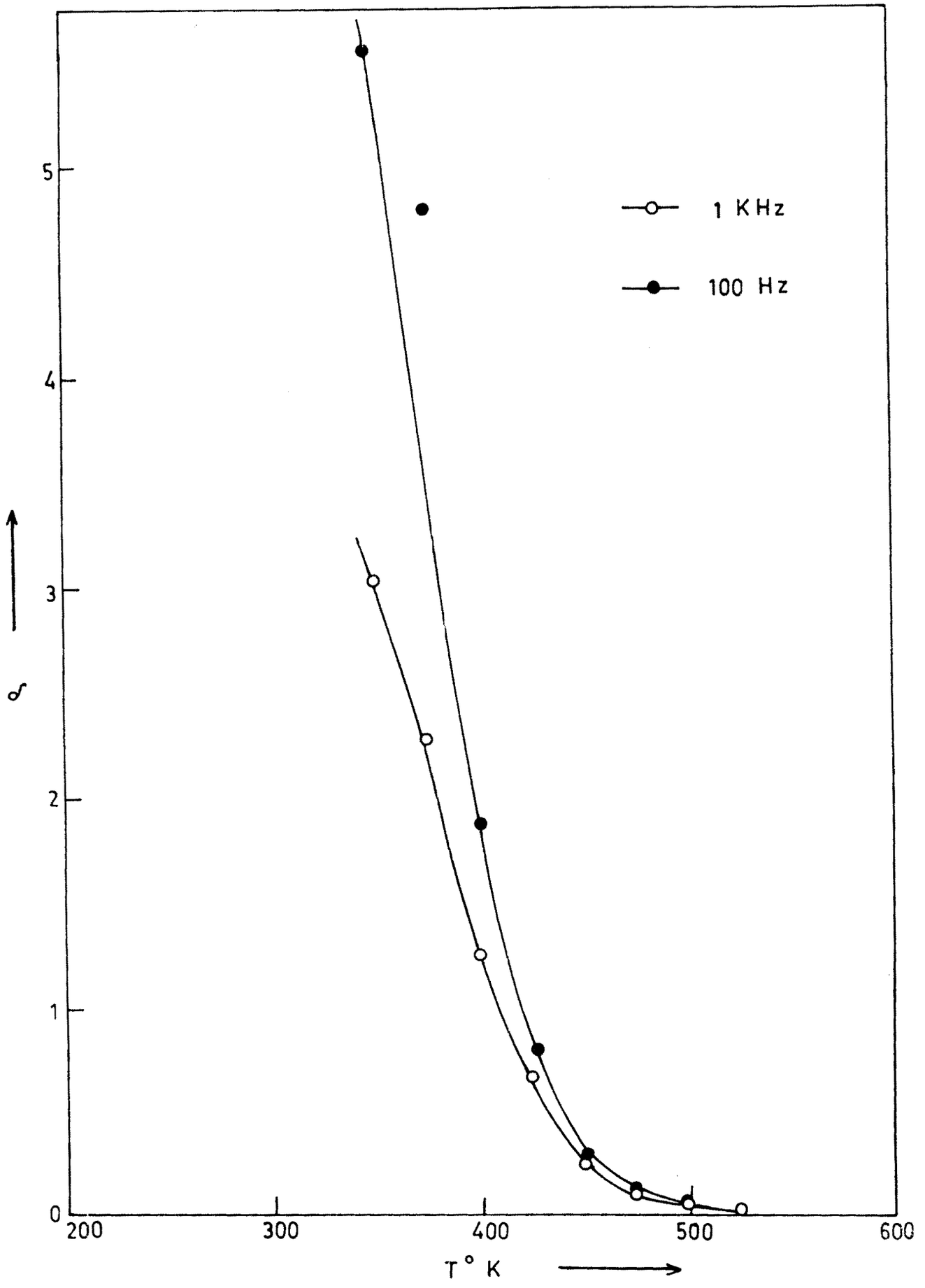

FIG. 4·2 – VARIATION OF RESISTIVITY WITH TEMPERATURE FOR B_3 FOR 100 Hz AND 1 KHz .

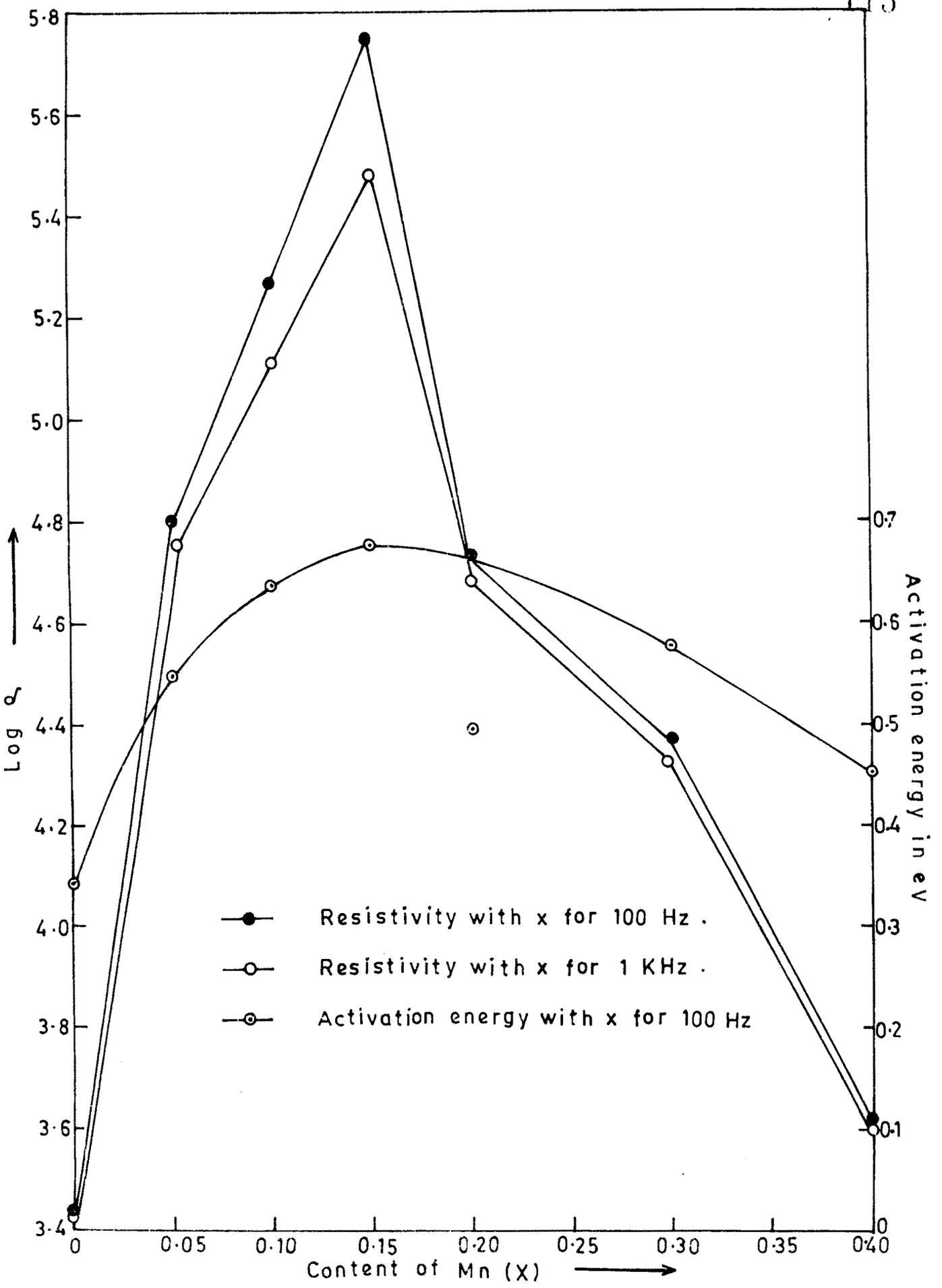

FIG. 4·3—VARIATION OF Log ρ , ACTIVATION ENERGY WITH CONTENT OF Mn .

TABLE 4.1

MEASUREMENTS WITH 100Hz OF RESISTIVITY, ACTIVATION ENERGY AND CURIE TEMPERATURE

Sample	Resistivity at 100°C in k-ohm-mtrs.	Activation Energy in		Curie temperature in °K.
		Para-region in eV	Ferri-region in eV	
B_1	2.762	0.2979	0.3476	636.9
B_2	63.682	0.3424	0.5518	598.8
B_3	187.104	0.4966	0.6357	657.89
B_4	561.392	0.5518	0.6754	649.35
B_5	53.551	0.6478	0.4966	574.71
B_6	23.398	0.5675	0.5822	549.45
B_7	4.133	0.5445	0.4551	487.8

TABLE 4.2

MEASUREMENTS WITH 1KHz OF RESISTIVITY, ACTIVATION ENERGY AND CURIE TEMPERATURE.

Sample	Resistivity at 100°C in k-ohm.mtrs.	Activation Energy in		Curie temperature in °K.
		Para-region in eV.	Ferri-region in eV.	
B_1	2.639	0.1986	0.3633	675.6
B_2	57.09	0.3660	0.9459	641.02
B_3	128.63	0.4110	0.6148	617.28
B_4	304.656	0.4966	0.6427	578.03
B_5	48.027	0.6273	0.3973	500.1
B_6	21.56	0.5463	0.5203	473.9
B_7	4.056	0.5518	0.3476	425.5

second region, conduction is greatly affected by the phase transition and in the third region, a hopping mechanism of conduction is suggested.

The variation of d.c. resistivity[19] with temperature can be attributed to ionic drift current, current due to electron hopping and current due to electrons in the conduction band. The current due to ionic drift is known to increase the resistivity with an increase in temperature, whereas current due to electron hopping and electrons in the conduction band results in a decrease of resistivity with temperature. This anamalous behaviour was observed in Tin and Zinc substituted Ni ferrites. The present results indicate that the contribution from the ionic drift current is not prominent whereas the last two mechanisms are more effective.

A typical figure 4.2 shows the variation of resistivity with temperature for B_3 sample. The a.c. resistivity is found to be lower than d.c. at lower temperatures. Therefore one can expect that electronic as well as ionic contributions are present in ρd.c. At higher temperatures ρd.c. and ρa.c. coincide indicating that the electronic charge carrier mobility and concentration become much larger than the mobility and concentration of the free ions. Hence, the ionic contribution becomes negligible and therefore, ρa.c. becomes entirely electronic at higher temperatures.

The activation energy as a function of Mn, is shown in the figure 4.3. Higher values of activation energy have been found to correspond to high resistivity values of the samples. In our case, the activation energy and resistivity increase upto 0.15 and

then both decrease. The activation energy values are in the range of 0.3 to 0.7 eV.

The conductivity in ferrites has been associated with the presence of ions of given element in more than one valence states. These ions get distributed over the crystallographically equivalent sites. The high conductivity of Fe_3O_4 is due to the low values of activation energy to cause normal electron hopping which are of the order of 0.2 eV and less. The high values of activation energy for our samples suggest that the hopping process due to polarons is favoured. Mostly theory of conductivity in ferrites has been explained on the hopping of polarons due to thermal activation.

In ferrites having the spinel structure the BB distances are smaller than AA and AB distances. However, BB distance is much larger than the sum of ionic radii of cations involved, indicating little or no overlap between 'd' wave functions of ions on adjacent octahedral sites. This gives rise to a situation in which the electrons are not free to move through crystal, but remain fixed on B-sites necessiating a hopping process. Result of conduction by hopping process is to increase effective mass and low mobility to current carriers. In this case the conduction can possibly be attributed to change of electrons between $Fe^{2+} \rightarrow Fe^{3+}$, $Ni^{2+} \rightarrow Ni^{3+}$, $Fe^{2+} + Mn^{3+} \rightarrow Fe^{3+} + Mn^{2+}$ and $Ni^{3+} + Mn^{2+} \rightarrow Ni^{2+} + Mn^{3+}$. Formation of such ions depends on the sintering condition and substitution.

For our system the cation distribution is given, $Zn_{.3}Fe_{.7}(Ni_{.7+x}Mn_xFe_{1.3-2x})O_4$. A-A hopping does not exist as there are only Fe^{3+} ions on this sublattice and any Fe^{2+} ion formed during processing preferentially occupies the B-site. Therefore,

B-B hopping is more predominant. Thus the reduction of Fe^{3+} ions on addition of Mn^{4+} ions is responsible to change the resistivity. The possibilities of formation of $Ni^{2+} \rightarrow Ni^{3+}$, $Mn^{4+} \rightarrow Mn^{3+}$ and Mn^{2+} must be taken into consideration for explaining the resistivity behaviour.

Addition of ions with incomplete 3d and 4s shells like Sc^{3+}, Ti^{4+} and V^{5+} usually leads to an increase in resistivity.[20] They act as electrostatic traps for exchange of electrons between Fe^{2+} and Fe^{3+} ions. When they are at octahedral sites, they can also act as scattering centres. These effects lead to an increase in resistivity. Ferric ions are also reported to be converted to ferrous ions on addition of tetravalent ions as $2Fe^{3+} \rightarrow Fe^{2+} + Mn^{4+}$. The resistivities are expected to increase due to localization of Fe^{2+} ions and the addition of Mn^{4+} results in overall decrease of Fe^{3+} from the ferrite material. This explains the increase of resistivity.

Electrical conduction in our samples may be due to the exchange of electrons between the Mn^{3+} and Mn^{4+} ions. Such exchange gives rise to an interesting trapping effect due to local Jahn-Teller distortions around Mn^{3+} ions. Around an Mn^{3+} ion(d^4 electronic configuration) the six oxygen ions are not equidistant from the central ion, the two being at a larger distance than the rest four. On the other hand, the six oxygen ions around an Mn^{4+} ion (d^3 configuration) are equidistant from the central ion. In such a case, when an electron jumps from an Mn^{3+} ion to the neighbouring Mn^{4+} ion, the new Mn^{4+} ion formed at the old site of the Mn^{3+} will be surrounded by the tetragonally distorted octahedron of the oxygen ions. Similarly the new Mn^{3+} will be surrounded by the

cubic octahedron of the oxygen ions. Both these arrangements are energetically unstable and a rearrangement of the oxygen ions has to take place. Thus each electron jump is associated with the movement of a large number of oxygen ions. This makes the movement of electron from one site to another more difficult and leads to a Jahn-Teller trapping. This would give - rise to an additional activation energy for the mobility. This type of behaviour of resistivity is seen in copper manganite, studied by Sabane et al.[21]

Electrical properties of Mn-Zn ferrites were studied by R.K.Puri et al.[22] As the concentration of Mn increases, Fe^{3+} - ions start migrating from octahedral to tetrahedral sites. It increases hopping of electrons in tetrahedral sites and this decreases the resistivity. It is also suggested that the conduction can possibly be attributed to exchange of electrons between $Fe^{2+} \rightarrow Fe^{3+}$, $Ni^{2+} \rightarrow Ni^{3+}$ and $Mn^{2+} \rightarrow Mn^{3+}$ ions. Since our samples are sintered in air and during cooling process, - oxidation and reduction of iron ions are possible, above processes may be responsible for the decrease in resistivity.

SECTION-B

DIELECTRIC CONSTANT

4.6. DIELECTRIC CONSTANT AND A.C.

The d.c. resistance of a polycrystalline material must necessarily be corroborated by the a.c. resistance and dielectric constant, so that it represents completely the conduction in the bulk of material. Dielectric losses occur in the electric polarization within the lattice at high frequencies. The

loss may be from imaginary component of dielectric constant and may be indistinguishable from other losses, such as losses in conduction.

Koops has given a general model for inhomogeneous dielectric and which comprises of well conducting grains that are separated by low conducting layers, leading to an equivalent parallel resistor and capacitor circuit. He studied the dispersion of resistivity and dielectric constant of some semi-conductors at audio frequencies. Van Uitert and Miles[23] reported that polycrystalline materials show that dielectric constant is frequency dependent and it exhibits dispersion with frequency. The a.c. resistivity shows the similar behaviour.

The Mn-Zn ferrites exhibit such dispersion and it can be explained on the basis of the assumption that ferrite compact consists of many layers. These layers constitute a condenser in which ferrite grains and boundaries possess different properties.

Murthy et al[24] and Habery et al[25] studied the Ni-Zn ferrites along with other ferrites. There is a correlation between dielectric constant behaviour and conduction mechanism. The spinel ferrites exhibit decreasing dielectric constant with increase in frequency in a certain range and it shows dispersion.

4.7. DIELECTRIC CONSTANT AND POLARIZATION

The dielectric displacement found in a dielectric when subjected to alternating electric field E, is given by $D = \epsilon^* E$ where ϵ^* is dielectric constant of dielectric material. This

dielectric constant is complex in nature, as response given to electric field is not instantaneous. The complex dielectric constant can be represented as, $\epsilon^* = \epsilon' - i\epsilon''$ where ϵ' is the real part and ϵ'' is the imaginary part of dielectric constant. The time lag responsible for complexity between the response and stimulus is represented by phase angle δ and for small values of phase angle, $\tan\delta = \epsilon''/\epsilon'$. As E depends on frequency and time, the real and imaginary parts of dielectric constant depend on frequency and time and it is necessary to study the dielectric properties of the material ϵ', ϵ'' and $\tan\delta$.

When a.c. electric field is applied to a sample, it gets polarized. The polarization can be electronic, ionic, orientational and space charge or interfacial. The observed polarization is the vector sum of the constituent polarizations.

4.8. EXPERIMENTAL TECHNIQUE

The measurements of capacitance C and dispersion factor D are carried out in Electronic Testing and Development Corporation, Peenya, Bangalore with pellets in frequency range - 1KHz to few MHz. 4192 A Hewlett Packard LF Impedance Analyzer of range 5Hz to 13MHz was used for this purpose. For good - contact of pellet, silver paste was applied on the opposite - faces of pellet and it was sandwitched between the copper foils, to which connecting leads were used.

Before taking the readings for capacity C and dispersion D, HP Impedance analyzer was made on for an hour and then was used for noting the measurements for various frequencies. By using

the relation $\epsilon' = Cd/\epsilon_o A$, the real part of dielectric constant was calculated. Here, C = capacity in farads, A = area in Mtr^2, d = thickness in mtrs and $\epsilon_o = 8.85 \times 10^{-12}$ mks units for free space are used. Also $\epsilon'' = \epsilon'.\tan\delta = \epsilon'.D$ is calculated for each frequency.

4.9. RESULTS AND DISCUSSION

In table 4.3 the values of dielectric constant, the dielectric loss and dielectric loss tangent obtained at 5KHz are given. The sample composition and the resistivity at 100°C are also included. The ϵ', ϵ'' and $\tan\delta$ decrease upto x = 0.1 and then increase with x. D.C. resistivity shows the reverse behaviour. Rezlescu *et al*[26] and Reddy *et al*[27] have studied the composition dependence of copper containing mixed ferrites and nickel substituted lithium ferrites respectively. They explained the composition dependence of dielectric constant by using the assumption that the mechanism of dielectric polarization is similar to that of conduction. The electron exchange interaction $Fe^{2+} \rightleftharpoons Fe^{3+}$ results in a local displacement of electrons in the direction of electric field which determines the polarization.

A similar mechanism is taken into consideration to explain the observed results in the present investigation. C. Prakash and Baijal[28] have observed similar results for Ni-Zn ferrites. The ions that take part into ion exchange can be produced during sintering process.[29] When the Ni containing ferrites are cooled from an elevated firing temperature in an oxidising atmosphere, a considerable amount of oxygen is observed and Ni^{3+} ions are formed. The formation of very small amount of Fe^{2+}

TABLE 4.3

DIELECTRIC DATA FOR THE SOLID SOLUTIONS OF $Zn_{.3}Ni_{.7+x}Mn_xFe_{2-2x}O_4$ AT 5KHz.

Composition	Dielectric constant '	Dielectric loss "	Dielectric loss tangent tan .	D.C. resistivity at 100°C in Kilo-ohm-mtrs.
$Zn_{.3}Ni_{.7}Fe_2O_4$	534.8	1524.8	2.85	2.762
$Zn_{.3}Ni_{.75}Mn_{.05}Fe_{1.9}O_4$	61.78	45.47	0.736	63.682
$Zn_{.3}Ni_{.8}Mn_{.1}Fe_{1.8}O_4$	30.85	-	-	187.104
$Zn_{.3}Ni_{.85}Mn_{.15}Fe_{1.7}O_4$	75.87	93.62	1.234	561.392
$Zn_{.3}Ni_{.9}Mn_{.2}Fe_{1.6}O_4$	70.91	82.89	1.169	53.551
$Zn_{.3}Ni_1Mn_{.3}Fe_{1.4}O_4$	104.44	133.89	1.282	23.398
$Zn_{.3}Ni_{1.1}Mn_{.4}Fe_{1.2}O_4$	516.14	1307.89	2.534	4.133

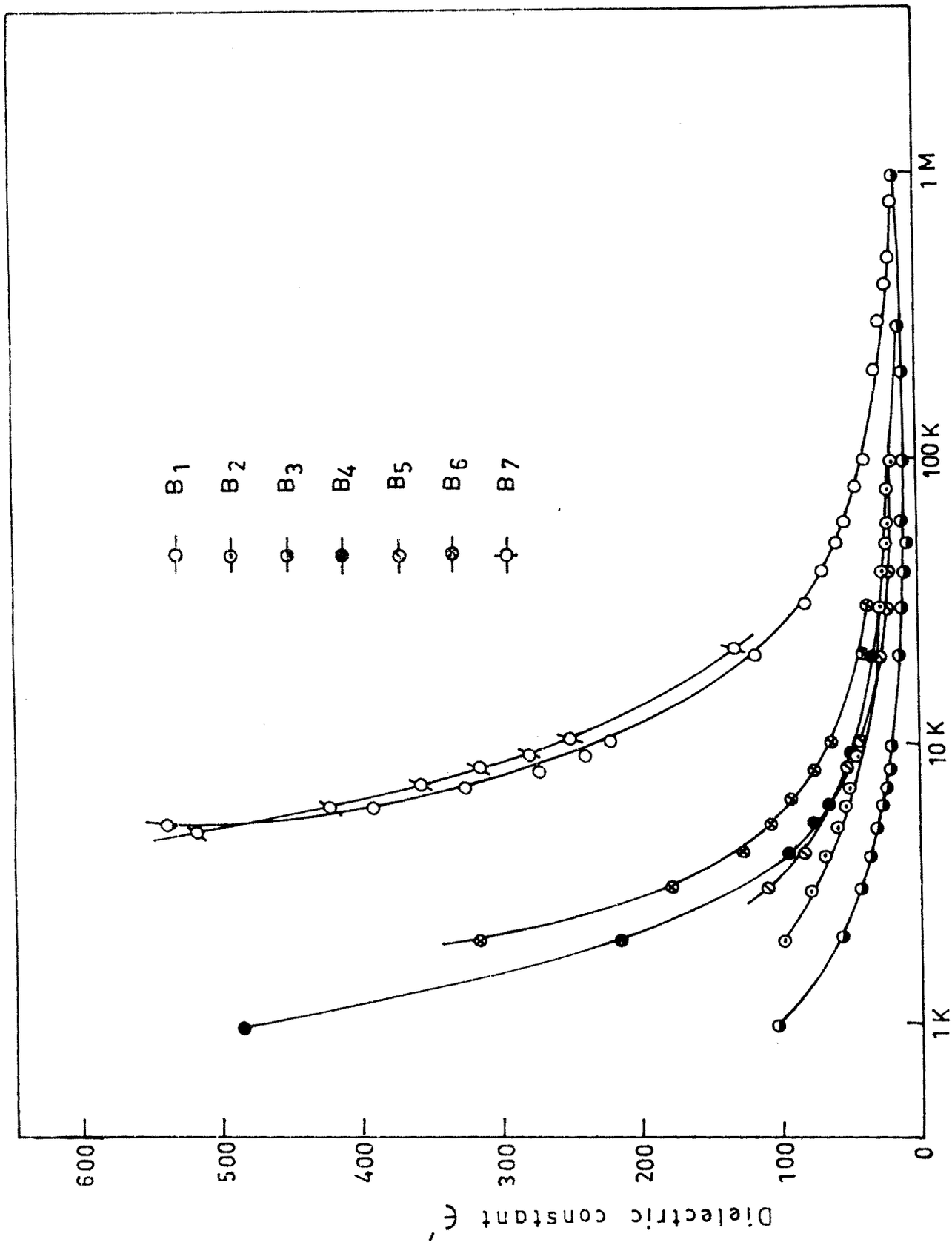

FIG. 4.4 — VARIATION OF DIELECTRIC CONSTANT WITH FREQUENCY.

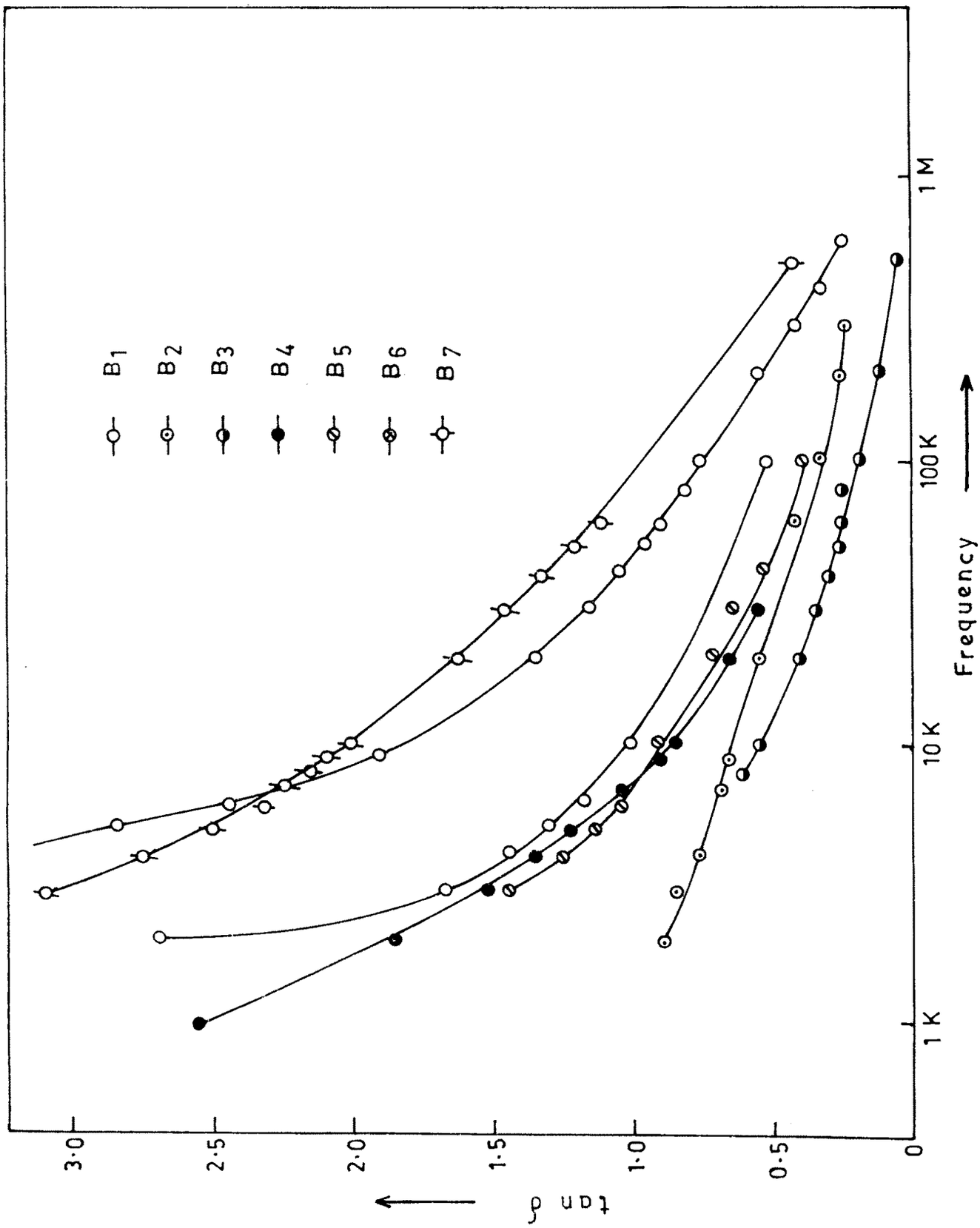

FIG. 4·5 — VARIATION OF tan δ WITH FREQUENCY.

ions due to volatalization of Zn during the sintering process is observed. It is also known that a partial reduction of Fe^{3+} ions to Fe^{2+} ions can take place at elevated firing temperature. The excess ions of Ni^{2+} and Mn^{4+} in the present system, may form as Ni^{3+} and Mn^{3+}. However formation of Mn^{3+} has been observed at higher content of Mn in ferrites. So the conduction may take place through electron exchange between Ni^{2+} and Ni^{3+}, Fe^{2+} and $Fe^{3+}$and Mn^{3+} and Mn^{4+} in the present system. The cation distribution of Mn substituted Ni-Zn ferrite with the general formula is given as, $Zn_{.3}Fe_{.7}(Ni_{.7+x}Mn_xFe_{1.3-2x})O_4$.

It is clear from the cation distribution that for the sample x = 0, the iron concentration is maximum at the octahedral site. Hence, the number of Fe^{2+} ions for the electron - exchange on octahedral sites is maximum. Therefore a comparatively high value of dielectric constant is observed. The substitution of 'x' Mn^{4+} ion changes the Fe ion concentration from 1.3 to 1.3-2x and Ni concentration from 0.7 to 0.7+x. - This decreases ferrous ions on the octahedral site which are available for polarization with a consequent decrease in dielectric constant. It is also stated that the tetravalent ions like Mn and Ti present at octahedral site localize the Fe^{2+} - ions by forming stable electrical bonds with Fe^{2+} ion. It can be given as $2Fe^{3+} \rightarrow Fe^{2+} + Mn^{4+}$. This localization effect obstructs the electron exchange by reducing the effective number of free Fe^{2+} ions with a consequent decrease in dielectric constant.

The increase in dielectric constant at or above x = 0.1 - may be due to the formation of more number of Ni^{3+} ions. The

multivalent states of Mn and the cluster formation at grain boundaries are responsible for high value of dielectric constant. In Mg-Mn ferrite,[30] it is observed that the formation of Mn^{3+} takes place along with Mn^{2+} when the Mn content is increased. $MnFe_2O_4$ [31] when heated around 1020°C, it decomposes as spinel plus Mn_2O_3. It is this presence of Mn in multivalent state, the unexplored nature of ferrite grain that leads to complex dielectric structure. So it can be concluded that for $x \leq 0.1$ dielectric response is dominated by electron exchange, whereas for $x > 0.1$ the dielectric response is dominated by the complex nature of dielectric.

The variation of dielectric constant with frequency for the series is given in the figure 4.4. All the samples reveal dispersion due to Maxwell-Wagner interfacial polarization in agreement with Koop's phenomenological theory.[32] The variation of dielectric relaxation intensity is primarily governed by the change in the dielectric constant at low frequencies with Mn concentration. This is in close agreement with the results obtained with magnetite by Iwuchi.[33] The observed variation in the dielectric relaxation intensity can be explained on the basis of space charge polarization due to inhomogeneous dielectric structure. The space charge polarization is governed by the number of space charge carriers and the resistivity of the sample. Therefore the dielectric relaxation intensity is expected to decrease with Mn at $x \leq 0.1$ and then increases again for Mn greater than 0.1. The similar variation of tanδ with frequency is observed. All the samples show dispersion in tan δ with frequency.

REFERENCES

1. Miyata N. J. Phys. Soc. Japan 16, 206 (1961).
2. Van Uitert L.G. Proc. IRE. 44, 1294 (1956).
3. Iwauchi K. Japan J.Appl. Phy. 10, 1520 (1971).
4. Von Hippel A.R. in "Dielectric Materials and Applications." Chapman and Hall Ltd. London (1954).
5. Peters J. and Standley K.J. 'The dielectric behaviour of Mn-Mg ferrite. Proc. Phys. Soc. 71, 131 (1958).
6. Verwey E.J.W. and Heilman J. Chem. Phy. 15, 174 (1947).
7. Koops C.G. Phy. Rev. 83, 121 (1951).
8. Maizen S.A. Phy. Stat. Solidi (Germany) Vol.70/1, p-k 71(1982)
9. Heikes and Johnston W.D. J.Chem. Phy. 26, 582 (1957).
10 Frohlich H. Adv. Phys. 3, 325 (1954).
11 Frankel J. "Kinetic theory of liquids' Dover Ch.7 (1955).
12 Mott N.F, Gurney R.W. in 'Electronic Processes in ionic crystals'. Oxford University Press, London (1948).
13 Parker.R. Phil. Mag. 3, 853 (1958).
14 Kawai Y., Tanable M, and Oqawa T. Phy. stat. solidi (Germany) 55/1, p-k 119 (1979).
15 Klinger M.I. J. Phy. C (GB) 8(21) 3595 (1975).
16 Komar A.P. and Klivshin V.V. Bull. Acad. Sc. USSR Phys. 18, 96 (1954).
17 Verwey E.J.W, Haayman P.W. and Romejn F.C. J.Chem. Phys, 15, 181 (1947).
18 Ghani A.A, Etach A.I, Mohmed A.A. Proc.ICF(1980).
19 Usha Varshney and R.J.Churchill, R.K.Puri and R.G.Mendiratta. I.C.F.(5) Proc. P.255, (1989).
20 Jain G.C, Das B.K: Kumari.S. J.Appl.Phy.49, 2894(1978).

21 Sabane C.D, Sinha A.P.B. and Biswas A.B.
Ind. J. Pure Appl. Phys. 4 (1966).

22 Puri R.K, Vijay.K.Babbar, R.G.Mendiratta.
Proc. ICF(5) P.239, (1989).

23 Miles P.A., West Phal W.B. and Von Hippel A.
Rev. Mod. Phys. 29, 279 (1957).

24 Murthy V.R.K. and Sobhandari J.
Phys. Stat. Sol.(a) 36, K-133 (1976).

25 Haberey F. and Wijn H.P.J.
Phy. Stat. Soli. 26, 231 (1968).

26 Rezlescu N. and E.Rezlescu. Phy. Stat. Sol.(A)
23, 575 (1974).

27 Reddy P.V. and T.S. Rao. J.Less Common Metals. 86, 255(1982).

28 Prakash.C. and J.S.Baijal.
J.Less Common Metals. 107, 51 (1985).

29 Van Uitert L.G. J.Chem. Phys. 23, 1883(1955).

30 Powar J.I, S.R.Sawant, S.A.Patil and R.N.Patil.
Mat. Res. Bull. 17, 339 (1982).

31 Prakash C. and J.S.Baijal,
Solid State Commun. 50, 557(1984).

32 Koops C.G. Phys. Rev.83 121 (1951).

33 Iwauchi K. Jpn. J. Appl. Phys. 10, 1520(1971).